JMEPEG (2007) 16:208–212
DOI: 10.1007/s11665-007-9033-3

1059-9495/$19.00

Deformation Mechanisms of Ti-6Al-4V During Tensile Behavior at Low Strain Rate

M. Vanderhasten, L. Rabet, and B. Verlinden

(Submitted April 20, 2006; in revised form January 2, 2007)

A superplastic Ti-6Al-4V grade has been deformed at a strain rate of 5×10^{-4} s^{-1} and at temperatures up to 1050 °C. Structural mechanisms like grain boundary sliding, dynamic recrystallization, and dynamic grain growth, occurring during deformation, have been investigated and mechanical properties such as flow stress, strain hardening, and strain at rupture have been determined. Dynamic recrystallization (DRX) brings on a decrease in the grain size. This could be of great interest because a smaller grain size allows a decrease in temperature for superplastic forming. For DRX, the driving force present in the deformed microstructure must be high enough. This means the temperature must be sufficiently low to ensure storing of enough dislocation energy but must also be high enough to provide the activation energy needed for DRX and to allow superplastic deformation. The best compromise for the temperature was found to be situated at about 800 °C; this is quite a bit lower than the 925 °C referenced in the literature as the optimum for the superplastic deformation. At this medium temperature the engineering strain that could be reached exceeds 400%, a value high enough to ensure the industrial production of complex parts by the way of the superplastic forming. Microstructural, EBSD, and mechanical investigations were used to describe the observed mechanisms, some of which are concurrent.

Keywords grain growth, recrystallization, superplasticity, texture, Ti-6Al-4V

1. Introduction

Nowadays titanium alloys are widely used in industrial and aeronautical applications. Properties such as strength, toughness, fatigue behavior, corrosion resistance, biocompatibility are the main reason for this. The property discussed in this contribution is the superplastic behavior of Ti-6Al-4V, better known as the workhorse titanium alloy (Ref 1). Superplastic materials are polycrystalline solids which have the ability to undergo large strains prior to failure. As a general rule, the deformation temperature has to be superior to half of the melting temperature, while the strain rate must be situated in the range of 10^{-4} s^{-1} to 10^{-2} s^{-1} (Ref 2-4). The aeronautical grade of Ti-6Al-4V is superplastic roughly between 750 °C and 950 °C, and between strain rates between 10^{-4} s^{-1} and 5×10^{-3} s^{-1}. Some authors report optimal superplasticity at about 927 °C (Ref 5-7). In the present study, the tensile properties, the structural and crystallographic texture evolution during deformation between room temperature (RT) and 1050 °C have been investigated. The strain rate was fixed at 5×10^{-4} s^{-1}, known to be the optimal superplastic strain rate. Structural mechanisms like grain boundary sliding, dynamic recrystallization and dynamic grain growth have been investigated. In order to study recrystallization phenomena, particular attention has been paid to the evolution of grain size as a function of temperature and of deformation. For well chosen samples texture measurements were performed.

This article was presented at the AeroMat Conference, International Symposium on Superplasticity and Superplastic Forming (SPF) held in Seattle, WA, June 6-9, 2005.

M. Vanderhasten and **L. Rabet,** Royal Military Academy, Renaissancelaan 30, 1000 Brussels, Belgium; and **M. Vanderhasten** and **B. Verlinden,** Department of Materials Engineering, Katholieke Universiteit Leuven Kasteelpark, Arenberg 44, 3001 Heverlee, Belgium. Contact e-mail: mathieu.vanderhasten@rma.ac.be.

2. Materials and Methods

The material used for the current study was a commercial titanium alloy, TIMETAL® 6-4 Titanium Aero. In the as received state, it was annealed after hot and cold rolling into sheet of 1 mm thickness and an initial grain size of 8 μm. In order to determine the influence of temperature on the mechanical behavior of this alloy, tests were performed on a tensile machine equipped with a furnace with three independent zones (constant temperature length 300 mm) and controlled atmosphere. The samples are flat with a gauge length of 10 mm and a width of 6 mm. The temperature was varied between room temperature and 1050 °C. The universal testing machine was operated at a constant true strain rate of 5×10^{-4} s^{-1}. During each test, a nitrogen gas flow was introduced in order to prevent oxidation of the sample and formation of α-case at the specimen surface. After each test, samples were quenched to room temperature by the injection of nitrogen gas inside the furnace. The method developed by Katrakova (Ref 8) was used to prepare the samples for automated Electron Backscattered Diffraction (EBSD) measurements. These measurements were carried out in a Philips XL30 microscope and analyzed with the FEI (TSL) software. Grain size measurements were performed with the mean linear intercept technique. For the texture measurements, (0002) pole figures (α-phase) and (110) pole figures (β-phase) were measured using a SIEMENS DCIM 500 diffractometer.

3. Results and Discussion

Depending on the overall form of the tensile curves, four temperature domains were considered and allow for the identification of the different underlying deformation mechanisms.

3.1 RT-650 °C

Figure 1 presents the true stress-true strain curves of samples deformed in this domain. At room temperature, there is classical work hardening and the ductility is limited. With increasing temperature a gradual softening occurs and the post-uniform elongation increases. In this domain the microstructural changes as shown in Fig. 2 are only caused by the tensile deformation. Dynamic recovery becomes more prominent with increasing temperature, but no dynamic recrystallization occurs.

3.2 650-750 °C

In this domain the ductility is greater (see Fig. 3) than at the lower test temperatures, and is probably caused by grain boundary sliding (GBS), which is typical for superplastic behavior. Texture measurements (see last section) enabled confirmation of this hypothesis.

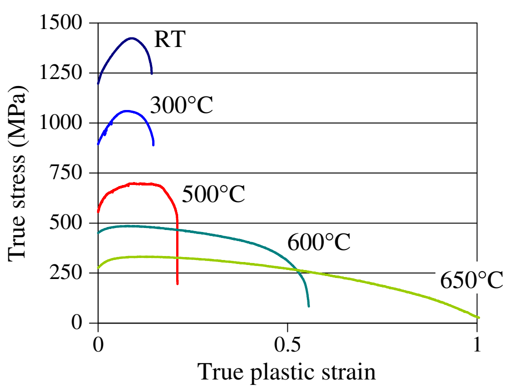

Fig. 1 True stress-true plastic strain curve of a Ti-6Al-4V flat specimen tested between room temperature (RT) and 650 °C with a strain rate o f5×10^{-4} s^{-1}

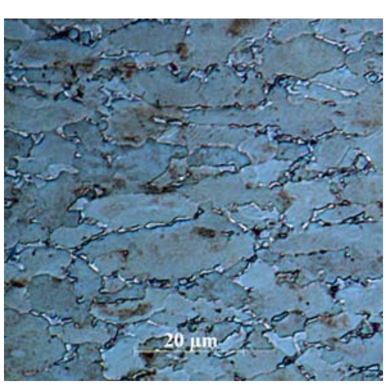

Fig. 2 Microstructure of a flat Ti-6Al-4V sample deformed at 500 °C at a strain rate of 5×10^{-4} s^{-1} until 30% engineering strain. (TD is the tensile direction)

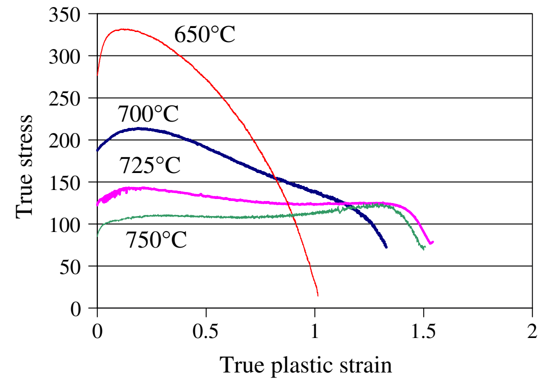

Fig. 3 True stress-true plastic strain curve of a Ti-6Al−4V flat specimen tested between 650 °C and 750 °C and a strain rate of 5×10^{-4} s^{-1}

The evolution of the grain size for deformation at 700 °C is shown in Fig. 4. A decrease in grain size of approximately 50% is observed in both the α- and β-phases. The decrease starts at about 10% engineering strain and stops at about 60%, where the grain dimensions seem to have stabilized.

The sample deformed for 30% exhibits a rather broad grain size distribution (Fig. 5). Some grains of the initial size (7-8 µm) are present together with smaller grains (2-3 µm). Samples quenched from 700 °C after different degrees of deformation show that the microstructure remains equiaxed during the whole deformation process.

Additional thermal treatments were performed to study the influence of deformation on the grain size evolution. First, undeformed samples were heated to 700 °C and maintained in the furnace during the same time as would be the samples during the tensile test. No variations were observed in the microstructure. Second, cold deformed samples were annealed during longer times between 8 and 24 min. After this heat treatment, the grain size decreased from 8 µm to 4 µm after 8 min and to 3 µm after 24 min (corresponding to the time to rupture of the tensile test at that temperature, the microstructure is presented at the Fig. 6). It can be clearly seen that the

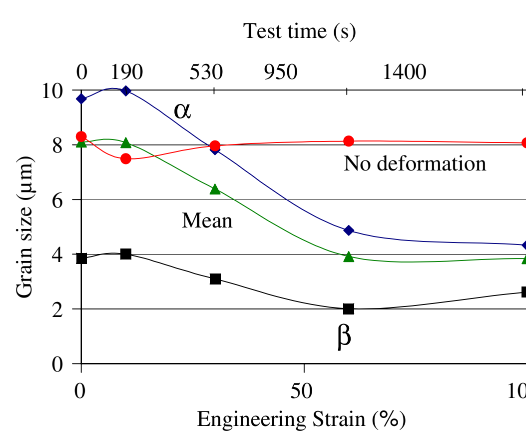

Fig. 4 Grain size evolution as a function of strain from a sample tested at 700 °C

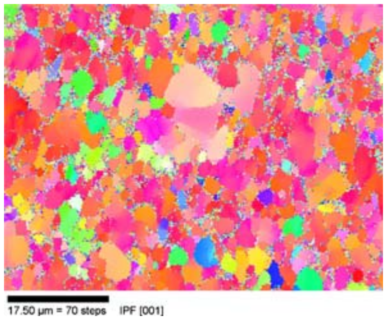

Fig. 5 Automated EBSD scan of a flat Ti-6Al-4V sample deformed at 700 °C at a strain rate of 5×10^{-4} s^{-1} until 30% engineering strain

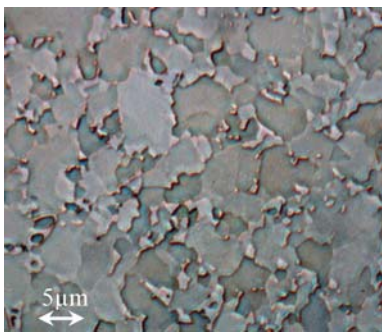

Fig. 6 Microstructure of a flat Ti-6Al-4V sample deformed at room temperature at a strain rate of 5×10^{-4} s^{-1} until 30% engineering strain and then heat treated 24 min at 700 °C

resultant microstructure is different from the one corresponding to the hot deformed sample; the grain size distribution is bimodal showing very smalls grains (approximately 1-2 µm) interspersed between larger grains 5-6 µm (see Fig. 6).

This difference in recrystallization kinetics indicates that hot deformation continues to provide the necessary driving force for the microstructural changes, and thus, one can conclude that the decrease in grain size is due to dynamic recrystallization. The observed phenomenon of dynamic recrystallization is quite similar with the one which was observed in commercially pure titanium by Zhu et al. (Ref 9).

3.3 750-950 °C

The evolution of the σ-ϵ curves as a function of temperature is presented in Fig. 7. At these temperatures, grain boundary sliding is active and deformation can be classified as "superplastic". The rupture strain is larger than at 700 °C but the material seems to undergo a kind of hardening. This is due to dynamic grain growth. To ensure material continuity during grain boundary sliding, some accommodation mechanisms, such as diffusion and dislocation climb, are needed. When the grain size increases, the importance of the accommodation also increases. On an σ-ϵ curve this will be evident by an increase in the flow stress.

At 800 °C the maximum rupture strain is obtained. The evolution of the grain size for this particular temperature is shown in Fig. 8. During the first part of the deformation, dynamic recrystallization occurs as in the previous temperature domain but gradually grain growth becomes more important.

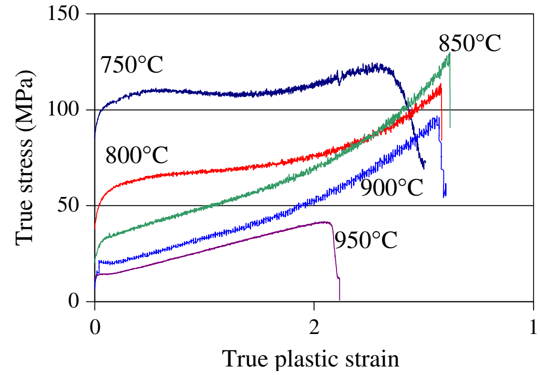

Fig. 7 True stress-true plastic strain curve of a Ti-6Al-4V flat specimen tested between 750 °C and 950 °C and a strain rate of 5×10^{-4} s^{-1}

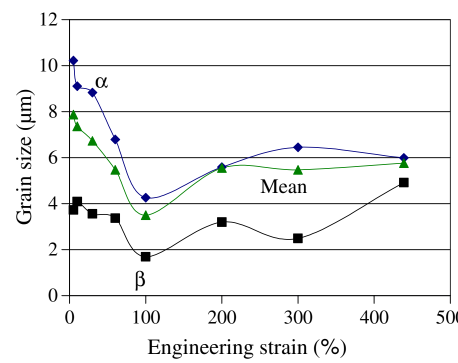

Fig. 8 Grain size evolution as a function of strain for a sample tested at 800 °C

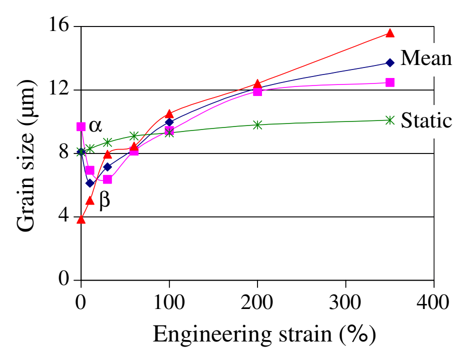

Fig. 9 Grain size evolution as a function of strain for a sample tested at 925 °C

This grain growth is mainly dynamic, and the influence of strain on grain growth is illustrated by thermal treatments at 800 °C. Without deformation only a slight variation of the grain size could be observed. Although the rupture strain starts decreasing clearly at about 900-925 °C, superplastic deformation is still active up to 950 °C. An explanation of this decrease can be found in the evolution of grain size as a function of strain at these temperatures. At 925 °C, grain growth become very pronounced in both phases, making the extent of DRX very limited and even difficult to observe (Fig. 9). At this temperature the static grain growth is clearly observed but it is

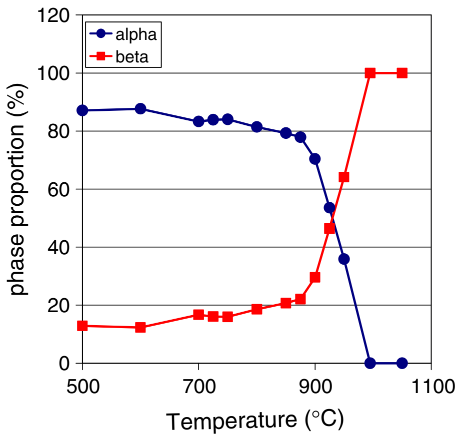

Fig. 10 Evolution of the phase proportions as a function of the temperature

still enhanced by the deformation. Grain boundary sliding was not observed directly on the deformed samples, nevertheless the fact that the flow stress increases with increasing grain size can be considered as indirect, but clear, evidence of its occurrence.

3.4 950-1050 °C

In this temperature domain, only DGG could be observed. The grains become too large for grain boundary sliding to occur. Another important point in this temperature interval is the proportion of β-phase. Superplastic deformation is favored by an equal amount of both α- and β-phase (Ref 10, 11). At 950 °C there is already 65% β-phase, and at 995 °C, the α-β transformation is complete (see Fig. 10). One sees that all parameters are negative for superplastic deformation, i.e., a large grain size and a predominance of β-phase.

In the literature, 927 °C is presented as optimum for superplastic deformation at a strain rate of 5×10^{-4} s^{-1} (Ref 5-7). In this study, superplastic deformation was effectively observed at this temperature but quite better results were seen at lower temperatures. The optimum was detected at about 800 °C where all parameters are favorable, indeed DRX caused grain refinement and not overruled by DGG. Also, this temperature is high enough to allow accommodation mechanisms to function and for GBS to be active. From an industrial point of view, it might be reasonable to work at 700 °C since rupture strain is high enough (350%) for most applications. A lower superplastic forming temperature would lead to worthwhile energy cost savings.

3.5 Texture Evolution

The texture evolution in both α- and β-phase has been determined. Comparing the as-received and hot deformed samples, no significant changes in β-phase texture were observed. On the other hand, the maximum intensity of the (0002) pole figure for the α-phase varies significantly. The as-received state (8.4 × random) decreases for a hot deformed sample at 600 °C to 2.2 × random, while for a sample deformed at 700 °C, the intensity drops to 4.1 × random after 100% strain before completely disappearing, probably due to grain boundary sliding (see Fig. 11).

4. Summary

The evolution of the mechanical behavior of Ti-6Al-4V with an initially equiaxed microstructure was investigated as a function of temperature at low strain rates. The microstructural evolution, and more particularly the grain size evolution, of the different phases have been determined by describing the phenomena taking place. The following conclusions are drawn from this work.

1. Between room temperature and 650 °C, deformation occurs by the conventional work hardening which is increasingly counterbalanced by recovery as temperature increases.
2. Between 650 °C and 750 °C, dynamic recrystallization and grain boundary sliding occur.
3. Between 750 °C and 950 °C, SP deformation is active but influenced by dynamic recrystallization and dynamic grain growth. At 800 °C all parameters are optimal for superplasticity.
4. Above 950 °C, dynamic grain growth is dominant, and causes, together with the increasing β-phase fraction, the disappearance of superplasticity.

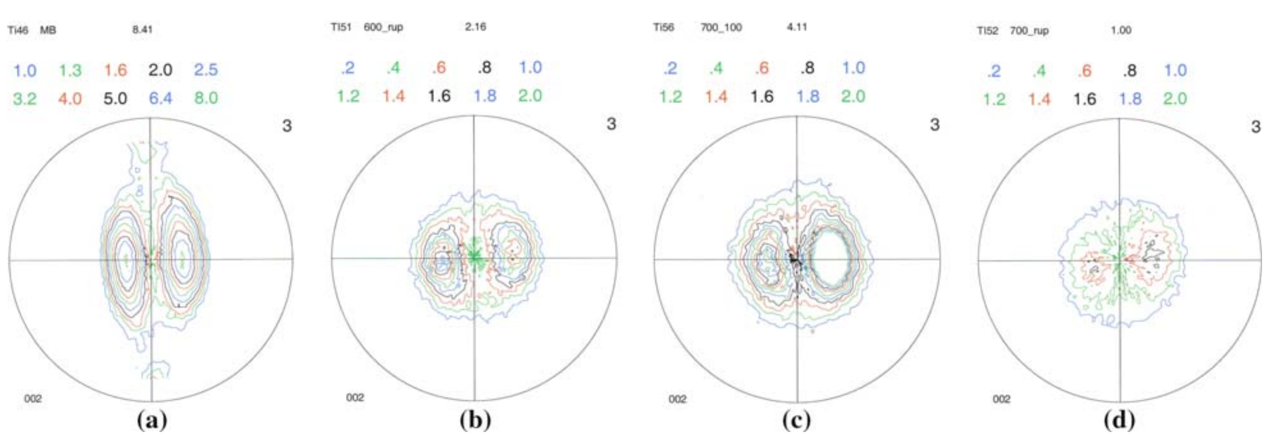

Fig. 11 (0002) pole figures for the α-phase (a) in the as-received state, (b) after rupture at 600 °C, (c) after 100% strain at 700 °C, and (d) after rupture at 700 °C (Ref 12)

Acknowledgments

This work was carried out in the frame of the "Inter University Attraction Poles program-Belgian Science Policy" under contract number IUAP P5-08, as well as the research project MX-03 of the BE Army Staff.

References

1. C. Leyens and M. Peters, Titanium and titanium alloys, Chichester (England): John Wiley & Son Inc., 2003, p 333–350
2. D.H. Avery and W.A. Backofen, A Structural Basis for Superplasticity, *Trans. Am. Soc. Met.*, 1965, **58**, p 551–562
3. R.H. Johnson, "Superplasticity," *Metall. Rev.*, 1970, **146**, p 115–134
4. W.B. Morrison, "The elongation of superplastic alloys," *Trans. Am. Inst. Min. Metall. Pet. Eng.*, 1968, **242**, p 2221–2227
5. A.K. Ghosh and C.H. Hamilton, "Mechanical Behaviour and Hardening Characteristics of a Superplastic Ti-6Al-4V alloy", *Metall. Trans. A*, 1979, **10A**, p 699–706
6. B.H. Cheong, J. Lin, and A.A. Ball, "Modelling of Hardening Due to Grain Growth for a Superplastic Alloy," *J. Mater. Process. Technol.*, 2001, **119**, p 361–365
7. C.H. Johnson, S.K. Richter, C.H. Hamilton, and J.J. Hoyt, "Static Grain Growth in a Microduplex Ti–6Al–4V Alloy," *Acta Mater.*, 1999, **47**(1), p 23–29
8. D. Katrakova, M.J. Damgaard, and F. Mücklich, "Structures of Trihydroxynaphthalene Reductase-Fungicide ComplexesImplications for Structure-Based Design and Catalysis," *Structure*, 2001, **38**, p 19–24
9. X.J. Zhu, M.J. Tan, and W. Zhou, "Enhanced Superplasticity in Commercially Pure Titanium Alloy," *Scripta Mater.*, 2005, **52**(7), p 651–655
10. M.L. Meier, D.R. Lesuer, and A.K. Mukherjee, "The Effects of the α/β Phase Proportion on the Superplasticity of Ti-6Al-4V and Iron-Modified Ti-6Al-4V," *Mater. Sci. Eng. A*, 1992, **154**(2), p 165–173
11. J.S. Kim, J.H. Kim, Y.T. Lee, C.G. Park, and C.S. Lee, "Microstructural Analysis on Boundary Sliding and its Accommodation Mode during Superplastic Deformation of Ti–6Al–4V Alloy," *Mater. Sci. Eng. A*, 1992, **263**(2), p 272–280
12. P. Van Houtte: The MTM-FHM Software System Version 2, Users Manual, 1995